DALTON
PERSPECTIVE

Methanol carbonylation revisited: thirty years on*

Peter M. Maitlis,[a] Anthony Haynes,[a] Glenn J. Sunley[b] and Mark J. Howard[b]

[a] *Department of Chemistry, The University of Sheffield, Sheffield S3 7HF, UK*
[b] *BP Chemicals Ltd., Hull Research and Technology Centre, Salt End, Hull HU12 8DS, UK*

Monsanto initiated development of its rhodium- and iodide-catalysed process for the carbonylation of methanol to acetic acid in 1966. Ownership of the technology was acquired in 1986 by BP Chemicals who have further extended it. The work of the Sheffield group, in developing a deeper understanding of the mechanism of the process, is reviewed. The rate-determining step in the rhodium–iodide catalysed reaction is the oxidative addition of methyl iodide to $[Rh(CO)_2I_2]^-$ **1a**: the product from this reaction, the reactive intermediate $[MeRh(CO)_2I_3]^-$ **2a** has been detected and fully characterised spectroscopically. The rates of the reversible reactions linking **1a**, **2a** and the acetyl complex $[(MeCO)Rh(CO)I_3]^-$ **3a**, as well as activation parameters for several of the processes involved, have been measured. The efficiency of methanol carbonylation arises primarily from rapid conversion of **2a** into **3a**, leading to a low standing concentration of **2a**, and minimising side reactions such as methane formation. By contrast, in the iridium-catalysed carbonylation, for which similar cycles can be written, the reaction of $[MeIr(CO)_2I_3]^-$ **2b** with CO to give $[(MeCO)Ir(CO)_2I_3]^-$ **4b** is rate determining. Model studies show that while k_{Rh}/k_{Ir} is *ca.* 1 : 150 for the oxidative addition, it is *ca.* 10^5–10^6 : 1 for migratory CO insertion. The migratory insertion for iridium can be substantially accelerated by adding either methanol or a Lewis acid (SnI_2); both appear to facilitate substitution of an iodide ligand by CO, resulting in easier methyl migration. The carbonylation of higher alcohols (ROH) has also been successfully modelled; the corresponding alkyl iodides (RI) react much more slowly than MeI with $[M(CO)_2I_2]^-$, but again give the acyls $[(RCO)M(CO)I_3]^-$ for M = Rh and the alkyls $[RM(CO)_2I_3]^-$ for M = Ir. The greater stability of $[MeIr(CO)_2I_3]^-$ compared with $[MeRh(CO)_2I_3]^-$ accounts for the very different characters of the reactions catalysed by the two metals. It is suggested that the broad features of the Rh/Ir reactivities can be rationalised since the M–C bond to a 5d metal is generally stronger than that to the corresponding 4d metal; thus if metal–ligand bond *making* plays a key role in a step, then the 5d metal is more likely to react faster (*e.g.* in the oxidative addition), but if a metal–ligand bond-*weakening* or -breaking step plays a key role in a process (*e.g.* in the migration), it is likely that the 4d metal will be faster.

The rhodium- and iodide-catalysed carbonylation of methanol to acetic acid is probably the most successful example of an industrial process homogeneously catalysed by a metal complex in solution that has yet been realised. A recent survey estimated that *ca.* 60% of the current world production of acetic acid (*ca.* 5.5 million tonnes per year) was made in this way, and virtually all new plants for acetic acid production now use this technology.[1]

The older alternative processes include the oxidation of fermentation ethanol (still used to make vinegar), acetaldehyde oxidation, followed later by oxidation of butane or naphtha. Significant cost advantages result from the use of carbon monoxide (derived from natural gas) as a feedstock and from the higher selectivity of methanol carbonylation processes. The first of these was commercialised in 1960 by BASF. It used an iodide-promoted cobalt catalyst but required very high pressures (600 atm) as well as high temperatures (230 °C), and gave *ca.* 90% selectivity (Table 1).[2]

The next major advance occurred in 1966 with the discovery by Monsanto of the rhodium- and iodide-catalysed reaction, which led to the start-up of their first commercial production unit in 1970.[3] The advantages over the cobalt-catalysed process are that significantly milder conditions (30–60 atm pressure and 150–200 °C) are employed, giving substantial savings in construction costs and hence in capital expenditure. The selectivity is also much better, leading to easier purification, and making further savings on both running and capital costs. One problem is that the process uses rhodium, a rare and very expensive metal, but a more significant disadvantage of all these carbonylation processes is that the reaction medium (acetic acid–HI at > 150 °C) is very corrosive, requiring the use of high cost, exotic materials for plant construction.

The reaction, which was then investigated by Forster and his co-workers at Monsanto,[4] represents one of the triumphs of modern organometallic chemistry. It is a classic example of a homogeneous catalytic process, made up of some six separate stoichiometric reactions, which link to form the cycle shown in Fig. 1.

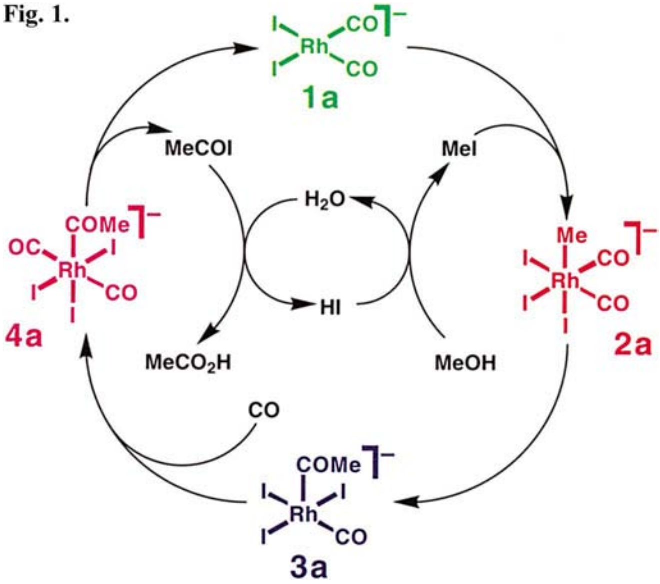

Fig. 1 Cycle for the rhodium- and iodide-catalysed carbonylation of methanol to acetic acid

---

* *Non-SI unit employed:* atm = 101 325 Pa.

Table 1 Comparison of reaction conditions and selectivity for commercial acetic acid processes

Process	Selectivity (% C per mol)	T/°C	p/atm
Naphtha oxidation (BP)	65–70	185	48
Methanol carbonylation, cobalt catalyst (BASF)	90	230	600
Methanol carbonylation, rhodium catalyst (Monsanto)	>99	150–200	30–60
Methanol–methyl acetate carbonylation, rhodium catalyst (BP)	High	150–200	30–50

The first step (reaction of methanol with HI to give methyl iodide) and the last (the reaction of acetyl iodide with water to give acetic acid and regenerate HI) are purely organic. Infrared spectroscopic studies *in situ* and under pressure showed that the major rhodium species present under catalytic conditions was $[Rh(CO)_2I_2]^-$ **1a**; kinetic measurements also showed that the rate of the overall reaction was first order in both [Rh] and [MeI] but zero order in [CO] and [MeOH]. The rate-determining step of the cycle was therefore suggested to be the oxidative addition of MeI to **1a**, to give $[MeRh(CO)_2I_3]^-$ **2a**. The model studies of Forster and co-workers[4] showed that in practice, the 'first' detectable product is the isomeric acetyl complex, $[(MeCO)Rh(CO)I_3]^-$ **3a**,* resulting from methyl migration. This monocarbonyl is then carbonylated to the six-co-ordinate dicarbonyl, $[(MeCO)Rh(CO)_2I_3]^-$ **4a**, that reductively eliminates acetyl iodide and regenerates $[Rh(CO)_2I_2]^-$ **1a**, which starts the whole cycle again.

In 1986 ownership of the Monsanto technology was acquired by BP Chemicals who have further developed the process and have licensed it around the world. BP have also extended the technology to the co-production of acetic anhydride and acetic acid, by carbonylation of methyl acetate and methanol, in their A5 plant at Hull in England, as has been described elsewhere.[1] A related catalytic system is used by Eastman to manufacture acetic anhydride.[6]

Sheffield Studies

This paper celebrates 30 years since the initial development of the process and discusses work carried out at the University of Sheffield in conjunction with BP Chemicals on elucidating further the mechanistic details of the catalytic cycle. Since catalytic reactions are, by definition, very fast, intermediates are rarely present in sufficient amounts to be readily detectable. Our approach has therefore been to separate the cycle into its component reactions and to study them individually, by measuring their rates and the effects of changes in conditions. Since the species involved are metal carbonyls which exhibit strong, characteristic infrared absorptions between *ca.* 2150 and 1600 cm^{-1}, a key tool for this work has been FTIR (Fourier-transform infrared) spectroscopy.

Some of the measurements could be carried out under conditions close to ambient, but many required higher temperatures and pressures, for which we used a cylindrical internal reflectance (CIR) infrared cell (Fig. 2). The CIR cell (Spectra-Tech), originally developed by W. R. Moser,[7] comprises a modified Parr reactor fitted with a CIR crystal (a silicon rod with polished conical ends) through which the IR beam from an FTIR spectrometer is transmitted. Internal reflections from the rod–solution interface lead to a modulation of the IR intensity by solvent and solute absorptions. The resulting IR spectrum is similar to that obtained from a conventional transmission cell but with a very short effective pathlength (*ca.* 10 μm). The cell is relatively straightforward to operate, allows the use of strongly absorbing solvents (such as water or acetic acid), and can be kept well stirred, ensuring homogeneous solutions.

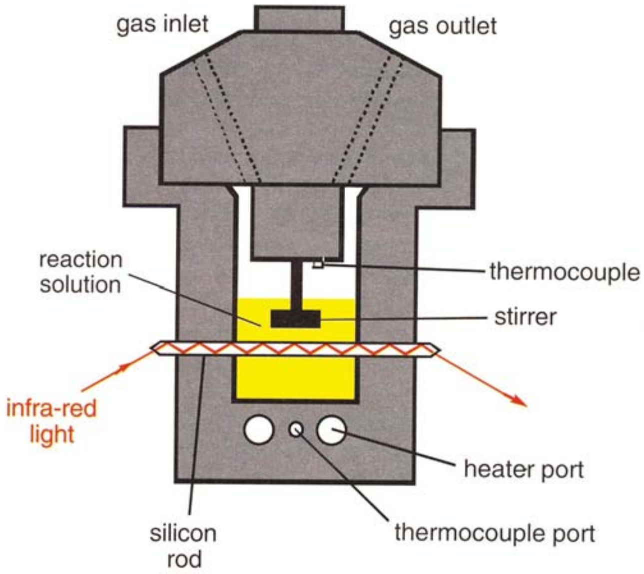

Fig. 2 Schematic diagram of the CIR cell used for infrared spectroscopic measurements at high temperature and pressure

A further essential tool in our armoury has been isotopic labelling (mainly with ^{13}C), which enables reaction pathways to be defined in more detail. The introduction of ^{13}C labels also allows the use of ^{13}C NMR spectroscopy to follow reactions and identify intermediates at low concentration.

Oxidative Addition of MeI to $[Rh(CO)_2I_2]^-$ 1a

The initial studies at Sheffield[8] focused on the reaction of MeI with $[Rh(CO)_2I_2]^-$, the rate-determining step in the cycle. The reaction was found to obey second-order kinetics (first order in [**1a**] and in [MeI]) and activation parameters were consistent with the classic S_N2 mechanism commonly proposed for addition of alkyl halides to square planar d^8 complexes. The reaction rate was found to show substantial dependencies on solvent, added salts and counter ion.

Protic solvents such as methanol accelerated the oxidative addition compared to aprotic solvents such as CH_2Cl_2 or methyl acetate. Addition of iodide salts (LiI or Bu_4NI) also led to enhanced rates, an effect which was suggested to be due to the formation of a highly nucleophilic dianion, $[Rh(CO)_2I_3]^{2-}$. However, our attempts to detect this species spectroscopically have so far failed; thus we now think that the effect of iodide is on the transition-state rather than the ground-state complex.

By contrast, counter ions containing NH groups (*e.g.* $C_{12}H_{25}NH_3^+$) inhibited oxidative addition, and spectroscopy[9] gave strong evidence for an interaction between the rhodium centre of **1a** and NH, thus reducing the nucleophilicity of the

---

* The X-ray structure determination[5] shows the acetyl complex to be dinuclear in the solid state with six-co-ordinate rhodium(III) and bridging iodides.

rhodium complex. Evidence was also obtained for the contact ion pair $[H^+ \cdots Rh(CO)_2I_2^-]$.

The Key Intermediate, $[MeRh(CO)_2I_3]^-$ 2a

All of the initial reactivity studies described in the previous section relate to measurements on the net reaction, **1a** + MeI ⟶ **3a**. However, although it was well established that this was the rate-determining step of the catalytic cycle, direct observation of the key first product of oxidative addition, **2a**, has only recently been accomplished, by precise choice of reaction conditions.[10]

When we followed the reaction of **1a** with neat MeI very carefully by IR spectroscopy, we observed a very weak ν(CO) peak at 2104 cm^{-1} (Fig. 3) which was not due to **1a**, **3a** or any other known rhodium–carbonyl–iodide species. This weak absorption appeared early in the reaction and then decayed in direct proportion to [**1a**], the behaviour expected for an intermediate. Comparison with spectra of the stable $[MeIr(CO)_2I_3]^-$ **2b** strongly suggested assignment of the 2104 cm^{-1} band to the high-frequency ν(CO) mode of the *cis*-dicarbonyl complex, $[MeRh(CO)_2I_3]^-$ **2a**. Using computer subtraction techniques, the low frequency ν(CO) band of **2a**, exhibiting identical kinetic behaviour, was located near 2065 cm^{-1} (Fig. 4), close to absorptions of **1a** and **3a**. The identity of the species responsible for these IR absorptions was confirmed by ^{13}C NMR spectroscopy on a sample prepared by dissolving **1a** in neat $^{13}CH_3I$ at low temperature. After brief warming to initiate, followed by recooling to freeze the reaction, the rhodium methyl-carbon resonance was observed at δ −0.65 [^1J(Rh–C) 14.6 and ^1J(C–H) 143 Hz] (Fig. 5) and the methyl protons at δ 2.08. A similar experiment using ^{13}CO-enriched **1a** allowed observation of a doublet at δ 175.9 [^1J(Rh–C) 59.9 Hz] due to equivalent carbonyl ligands in **2a**. The conditions (high concentrations of the reactants and a non-polar medium) for these experiments were chosen in the expectation that they would favour formation of a detectable quantity of the intermediate **2a**. The IR data indicate that under steady-state

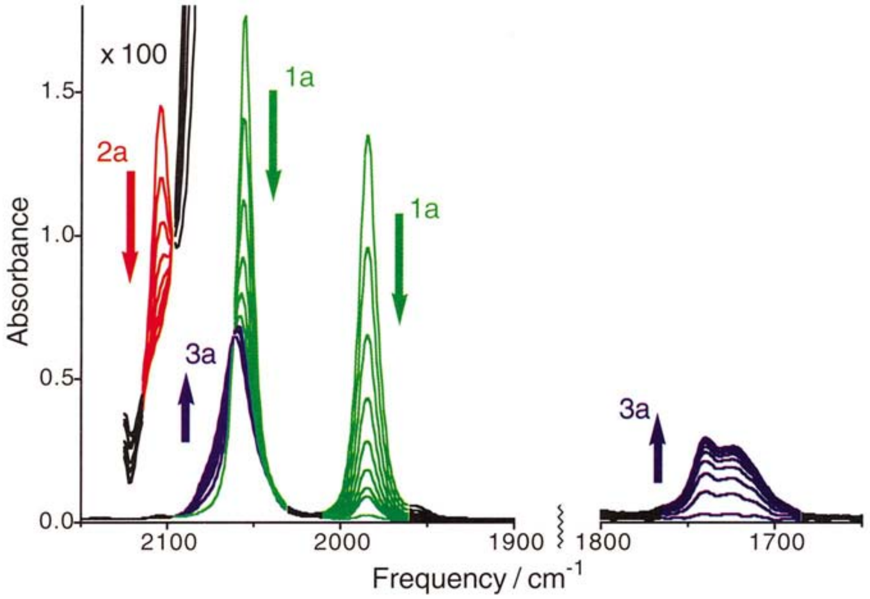

Fig. 3 A series of infrared spectra [ν(CO) region] recorded during the reaction of $Bu_4N[Rh(CO)_2I_2]$ with neat MeI at 25 °C. Note the weak band (at 2104 cm^{-1}, expanded 100 times) due to the intermediate **2a**

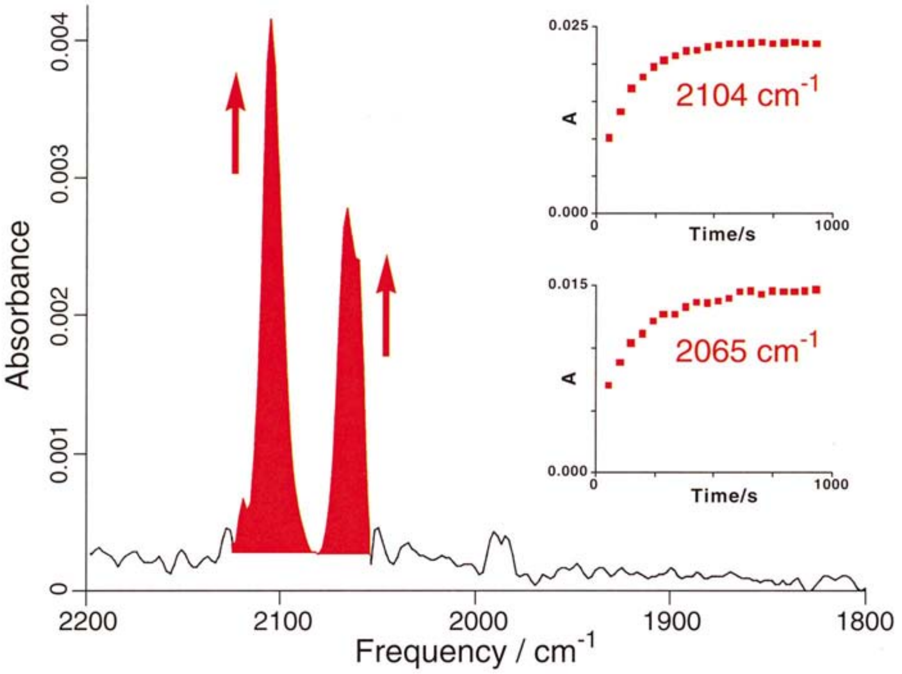

Fig. 4 Infrared spectrum [ν(CO) region] of **2a** generated by computer subtraction of bands due to **1a** and **3a**. The relative intensities are consistent with a *cis*-dicarbonyl. Inset are kinetic traces showing the growth of the two absorptions of **2a** in the initial stages of the reaction of $Bu_4N[Rh(CO)_2I_2]$ with neat MeI at 5 °C. Note that both bands appear at the same rate, indicating that they belong to the same species

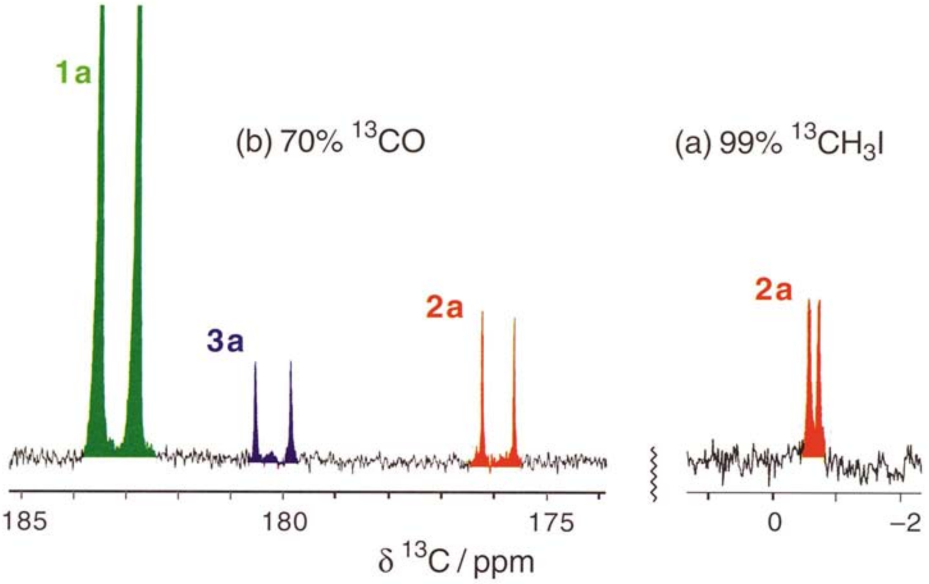

Fig. 5 Low-temperature ^{13}C NMR spectra (-50 °C) illustrating detection of signals due to the rhodium–methyl intermediate, **2a**, during the reaction of $\mathrm{Bu_4N[Rh(CO)_2I_2]}$ with MeI using (*a*) 99% ^{13}C-enriched MeI and (*b*) *ca.* 70% ^{13}CO-enriched rhodium complex. All the signals are doublets due to ^{103}Rh–^{13}C coupling

conditions in neat MeI the concentration of **2a** is *ca.* 1% of that of **1a**; this is also in agreement with estimates based on NMR intensities.

The IR spectrum of **2a** indicated that a *cis*-dicarbonyl rhodium(III) species was present, while the NMR data showed that the two carbonyl ligands were equivalent; both the IR and the NMR results were consistent with the *fac,cis* structure shown for **2a** in Fig. 1; the same geometry was also found by a crystal structure determination for the *n*-hexyliridium complex (Fig. 6, and see below).

The detection of **2a** allowed the determination of reactivity data by monitoring its kinetic behaviour using FTIR spectroscopy. At high MeI concentrations, pseudo-first-order conditions apply and application of the steady-state approximation to intermediate **2a** [equation (1)] leads to an expression for

$$\underset{\mathbf{1a}}{[\mathrm{Rh(CO)_2I_2}]} + \mathrm{MeI} \underset{k_{-1}}{\overset{k_1}{\rightleftharpoons}} \underset{\mathbf{2a}}{[\mathrm{MeRh(CO)_2I_3}]} \underset{k_{-2}}{\overset{k_2}{\rightleftharpoons}} \underset{\mathbf{3a}}{[\mathrm{(MeCO)Rh(CO)I_3}]} \qquad (1)$$

the observed rate constant for conversion of **1a** into **3a** [equation (2)]. Since the relationship between the concentrations of **1a** and **2a** is given by equation (3), k_2 can be expressed

$$k_{\mathrm{obs}} = \frac{k_1 k_2[\mathrm{MeI}]}{k_{-1} + k_2} \qquad (2)$$

$$\frac{[\mathbf{2a}]}{[\mathbf{1a}]} = \frac{k_1[\mathrm{MeI}]}{k_{-1} + k_2} \qquad (3)$$

as in equation (4). The rate constant k_{obs} can be measured

$$k_2 = k_{\mathrm{obs}}\frac{[\mathbf{1a}]}{[\mathbf{2a}]} \qquad (4)$$

directly and the ratio [**1a**]:[**2a**] can be estimated from relative IR intensities, based on a reasonable assumption concerning relative molar absorption coefficients. Thus the migratory insertion rate constant, k_2, is accessible.

In addition to measuring the rate of transformation of **2a** into **3a** (k_2) we were able to measure the rate of the reverse reaction (k_{-2}). Forster had already established[4] that on heating complex **3a** regenerated **1a** and methyl iodide, thus indicating the reversibility of both the oxidative addition and the methyl migration processes. Using specifically labelled $[\mathrm{(Me^{13}CO)Rh(CO)I_3}]^-$, in the *presence* of an excess of MeI to suppress reductive elimination and isolate the migration process, we were able to measure the first-order rate constant (*i.e.* k_{-2})

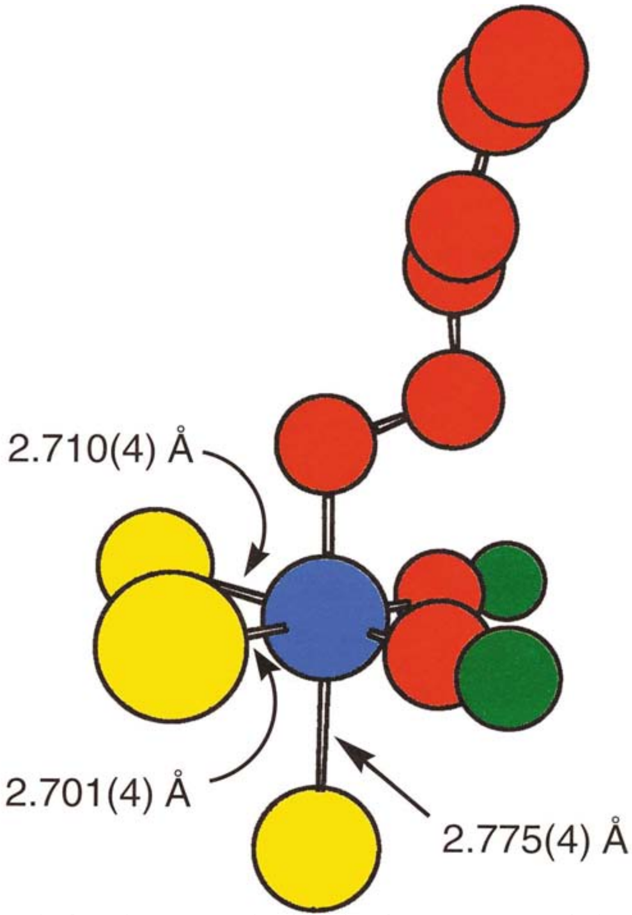

Fig. 6 Crystal structure showing the *fac,cis* geometry of the octahedral iridium anion in $\mathrm{AsPh_4[(\textit{n}\text{-}C_6H_{13})Ir(CO)_2I_3]}$. The tetraphenylarsonium cation has been removed for clarity. Note the difference in Ir–I bond lengths, indicating the high *trans* influence of the alkyl group

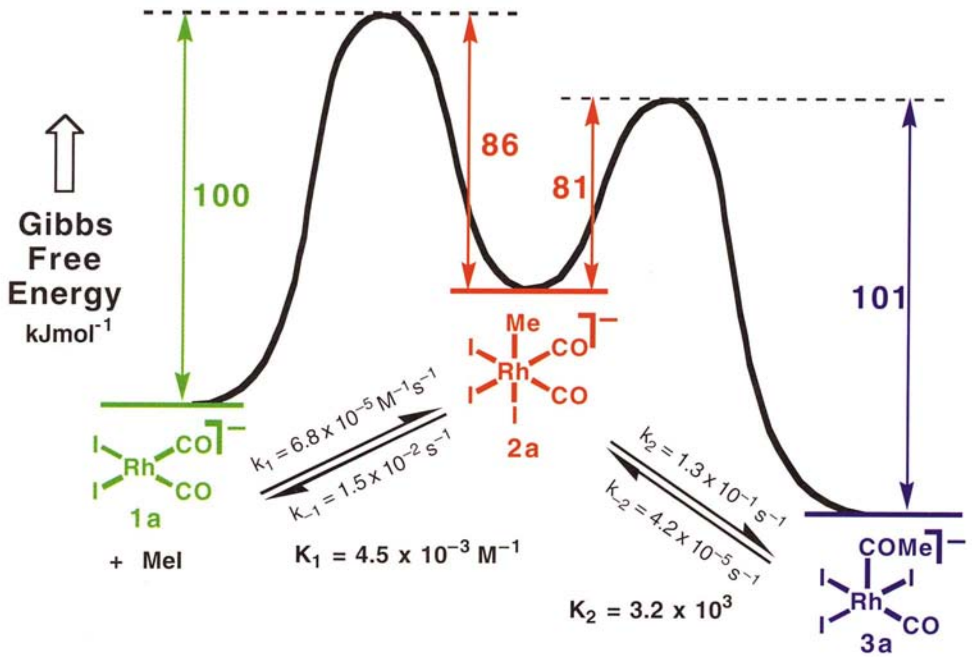

Fig. 7 Free energy profile constructed from kinetic data for interconversions of complexes **1a**, **2a** and **3a** at 35 °C in CH_2Cl_2–MeI. Equilibrium constants K_1 and K_2 calculated from the forward and reverse rate constants, are also given. Note that the rhodium–methyl intermediate, **2a**, is unstable with respect to *both* reductive elimination and methyl migration

for exchange of label between acetyl and terminal carbonyl positions. Comparison with the rate of the net reaction, **3a** ⟶ **1a** + MeI, in the *absence* of MeI allowed the estimation of k_2/k_{-1} (*ca.* 9 at 35 °C).* This showed that migratory insertion in **2a** is an order of magnitude faster than reductive elimination, and that the low steady-state concentration of **2a** during oxidative addition is primarily due to the rapid migratory insertion, and not to a fast back-reaction.

Complete rate data for the interconversions shown in equation (1) were thus obtained at 35 °C (Fig. 7), which allowed the calculation of the equilibrium constants K_1 and K_2. These show that **2a** is unstable with respect to both migratory insertion and reductive elimination.

Activation parameters measured for the k_2 and k_{-2} steps have allowed estimation of the thermodynamic data, ΔH° −37 kJ mol^{-1} and ΔS° −54 J mol^{-1} K^{-1} for isomerisation of **2a** to **3a**. The data predict that K_2 decreases markedly at higher temperatures and is *ca.* 30 in the range where the carbonylation reaction is operated. Thus **3a** becomes less favoured with respect to **2a** at higher temperatures; however, the trapping of **3a** by CO to give the dicarbonyl, **4a**, must be very efficient under catalytic conditions. The results also show that the high selectivity of the rhodium-catalysed process (particularly the low rate of methane formation) can be explained by the very small standing concentration of the methyl species, **2a**; this is due to both the rapid migratory insertion in **3a** and the unfavourable thermodynamics of MeI oxidative addition. This may be contrasted with the iridium system (see below).

Reductive Elimination from $[(MeCO)Rh(CO)_2I_3]^-$ 4a

The *mono*carbonyl acetyl complex, **3a**, decomposes by loss of methyl iodide rather than of acetyl iodide; however, addition of CO (a reversible process[11]) leads to the *di*carbonyl, **4a**, which reductively eliminates acetyl iodide to regenerate **1a**. This final organometallic step in the catalytic cycle has received less attention, but we find that decomposition of **4a** occurs quite slowly under ambient conditions ($t_{\frac{1}{2}}$ = 12 h at 25 °C in CH_2Cl_2). A recent study by the du Pont group[12] has shown that reductive elimination of acetyl iodide is reversible [equation (5)].†

$$[(MeCO)Rh(CO)_2I_3]^- \rightleftharpoons [Rh(CO)_2I_2]^- + MeCOI \quad (5)$$

The reductive elimination of acetyl iodide from **4a** is accompanied by side reactions arising from the extreme facility with which acetyl iodide undergoes hydrolysis by traces of water. This gives rise to HI, which reacts with $[Rh(CO)_2I_2]^-$ [equation (6)] to give a rhodium(III) tetraiodide complex.

$$[Rh(CO)_2I_2]^- + 2HI \longrightarrow [Rh(CO)_2I_4]^- + H_2 \quad (6)$$

Thus although traces of water lead to difficulties in measuring accurate kinetics for reductive elimination, approximate activation parameters ($\Delta H^\ddagger$ 87 kJ mol^{-1} and $\Delta S^\ddagger$ −43 J mol^{-1} K^{-1}) have been obtained. In addition, dramatic effects are observed on addition of other nucleophiles. For example, addition of 1 molar equivalent of tetrabutylammonium acetate to a solution of **4a** leads to immediate and quantitative formation of **1a** and acetic anhydride [ν(CO) 1825 cm^{-1}] [equation (7)].

$$[(MeCO)Rh(CO)_2I_3]^- + MeCO_2^- \longrightarrow [Rh(CO)_2I_2]^- + (MeCO)_2O + I^- \quad (7)$$

Secondary amines also react with **4a** to generate **1a**, this time with the formation of the corresponding amide [equation (8)].‡

---

* Kinetic data indicate that the reaction of methyl iodide with **1a** to give **3a** proceeds *ca.* 4 times as fast in methanol as in an aprotic solvent under comparable conditions (25 °C).[8] Closer analysis of a reaction of **1a** with methyl iodide showed that complex **2a** was still detectable on change of co-solvent from MeI–CH_2Cl_2 (80:20 v/v) to MeI–MeOH (80:20 v/v), and that k_1 was increased by *ca.* 50% and k_2 by *ca.* 100%. Thus, while a protic solvent does increase the rates both of the oxidative addition and of the migration reaction on rhodium, the effects seem to be comparatively modest.

† Carbon-13 NMR spectroscopy showed that oxidative addition of acetyl iodide to **1a** at low temperature gave *cis*-**4a** as the initial product. On warming, *cis*-**4a** isomerised to the more thermodynamically stable *trans*-**4a**, which is the isomer produced directly by carbonylation of **3a**. We have confirmed the du Pont observations by IR spectroscopy.

‡ The reactions are rapid at room temperature for dialkylamines (R^1 = R^2 = Et or Bu^n) but slower for the less nucleophilic *N*-methylaniline (R^1 = Ph, R^2 = Me). Diphenylamine gives no discernible increase in rate over that measured in the absence of nucleophile.

Table 2 Activation parameters for catalytic carbonylation processes and individual reactions from the catalytic cycles

Reaction	Ref.	$\Delta H^{\ddagger}$/kJ mol^{-1}	$\Delta S^{\ddagger}$/kJ mol^{-1}
Catalytic processes			
$MeOH + CO \longrightarrow MeCO_2H$ (Rh–I$^-$)	4	63.6	−116
$MeCO_2Me + CO \longrightarrow (MeCO)_2O$ (Rh–I$^-$)	6	60.2	−113
$MeOH + CO \longrightarrow MeCO_2H$ (Ir–I$^-$)	16	34	−246
Model reactions			
$MeI + [Rh(CO)_2I_2]^- \longrightarrow [MeRh(CO)_2I_3]^-$ (MeOH)	8	60	−120
$MeI + [Rh(CO)_2I_2]^- \longrightarrow [MeRh(CO)_2I_3]^-$ (CH_2Cl_2)	8	53	−150
$MeI + [Rh(CO)_2I_2]^- \longrightarrow [MeRh(CO)_2I_3]^-$ (MeI)	10	50	−165
$[MeRh(CO)_2I_3]^- \longrightarrow [(MeCO)Rh(CO)I_3]^-$ (MeI)	10	63	−59
$MeI + [Ir(CO)_2I_2]^- \longrightarrow [MeIr(CO)_2I_3]^-$ (CH_2Cl_2)	17	54	−113
$[MeIr(CO)_2I_3]^- + CO \longrightarrow [(MeCO)Ir(CO)_2I_3]^-$ (PhCl)	18	155	91
$[MeIr(CO)_2I_3]^- + CO \longrightarrow [(MeCO)Ir(CO)_2I_3]^-$ (PhCl–MeOH)	18	33	−197

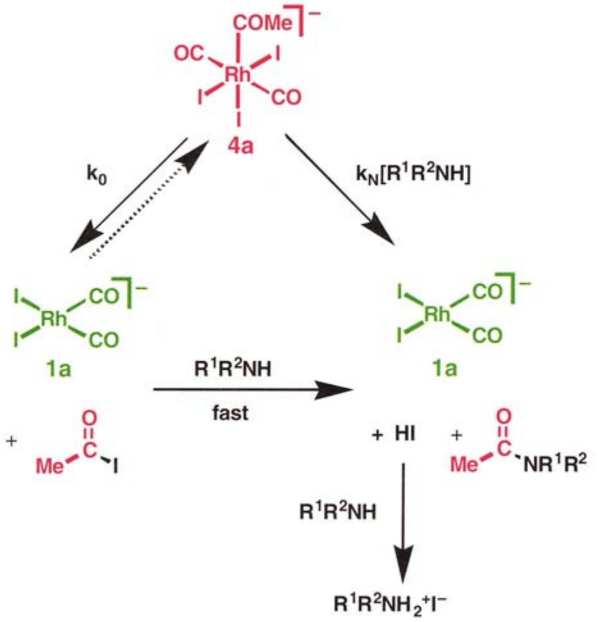

Fig. 8 Two pathways for the reaction of $[(MeCO)Rh(CO)_2I_3]^-$ **4a** with amines: (*i*) the unassisted reductive elimination (k_0 route) and (*ii*) direct nucleophilic attack by the amine (k_N route). Both routes lead to the same products, since acetyl iodide will react rapidly with the amine

$$[(MeCO)Rh(CO)_2I_3]^- + R^1R^2NH \longrightarrow [Rh(CO)_2I_2]^- + R^1R^2NCOMe + HI \quad (8)$$

Preliminary kinetic studies on the reaction with *N*-methylaniline suggest parallel first- and second-order pathways ($k_{obs} = k_0 + k_N[PhNHMe]$), which we interpret as evidence for direct nucleophilic attack on the rhodium acyl competing with unassisted reductive elimination (Fig. 8).[13] These observations suggest that direct attack by external nucleophiles at the bound acyl ligand can play a significant role in the reductive elimination process.[14]

Relation of the Individual Steps to the Overall Cycle

Our approach of dissecting the catalytic cycle into its component steps is validated by a comparison of activation parameters found for oxidative addition of MeI to **1a** with those determined by other workers for the overall carbonylation process (Table 2).[4,6,15] The parameters for the *model* reaction in methanol are particularly close to those for the *catalytic* reactions, and even though the stoichiometric oxidative addition is significantly slower in aprotic solvents the agreement is still reasonable.

It is interesting to compare reactivity data for the oxidative addition of MeI to **1a** with that for the reductive elimination **4a** ⟶ **1a** + MeCOI. We estimate that in dichloromethane containing 1 mol dm^{-3} MeI the two reactions will have equal rates at *ca.* 30 °C. Above this temperature the oxidative addition is rate limiting, whilst below it the reductive elimination would be the rate-determining step of the cycle. This demonstrates how changes in reaction conditions can lead to dramatic consequences for the rate-determining step of a catalytic process.

Since oxidative addition to a rhodium(I) centre 'controls' catalytic activity under normal operating conditions, it should be possible to accelerate the process by making the rhodium centre more nucleophilic, for example by the addition of phosphines or other electron releasing ligands.[19] It has recently been found that chelating ligands containing both phosphorus and sulfur donors lead to enhanced catalytic activity in batch reactions.[20] The main problem with these modified systems is the long term stability of the complex and the ligand under process conditions.

Comparisons with Iridium

Other Group VIII metals have been reported to be active for methanol carbonylation, and in their original work the Monsanto group noted the effectiveness of iodide-promoted iridium catalysts.[3,4] This has been confirmed by other workers,[16] and thus it is instructive to compare the kinetics and mechanism of catalysis for the rhodium and iridium systems.

Forster's mechanistic studies of iridium-catalysed methanol carbonylation showed many similarities to the rhodium system, but with a greater degree of complexity, due to the participation of both neutral and anionic species.[21] High-pressure IR spectroscopic studies showed that the main species present were the iridium(III) complexes, $[MeIr(CO)_2I_3]^-$ **2b**, which is 'active', and $[Ir(CO)_2I_4]^-$. The latter is 'inactive' and needs to be reduced to **1b** before it can further participate in the methanol carbonylation cycle. A similar inactive species, $[Rh(CO)_2I_4]^-$, forms in the rhodium-catalysed reactions, but this is more easily reduced and is therefore less troublesome.

A simplified version of the 'anionic' iridium cycle is shown in Fig. 9. The principal difference between rhodium and iridium is a change in the rate-determining step. Oxidative addition of MeI to the iridium(I) anion, **1b**, is fast, the slow step now being the carbonylation of **2b** to give **4b**. In contrast to the rhodium system, where specially chosen conditions were required to detect the rhodium–methyl complex **2a**, salts of the iridium analogue, **2b** are stable and isolable, and there is no tendency for spontaneous isomerisation to an acetyl complex.[*,22] A

---

[*] The complex **2b** shows a ^1J(C–H) of 139 Hz for the methyl attached to iridium,[23] this agrees well with the value reported for ^1J(C–H) of 143 Hz for the methyl attached to rhodium in the intermediate **2a**.

crystal-structure determination[17] of the *n*-hexyliridium analogue $[(n\text{-}C_6H_{13})Ir(CO)_2I_3]^-$ (from oxidative addition of *n*-iodohexane to **1b**) shows it to have the *fac,cis* octahedral geometry (Fig. 6). Kinetic measurements for the reaction of MeI with **1b** gave the activation parameters (Table 2), and direct comparison of rate data shows that oxidative addition of methyl iodide is 120 times faster for iridium than for rhodium in CH_2Cl_2 at 25 °C.[24]

By contrast to the rapid methyl migration in the rhodium system, Forster found that **2b** reacted only slowly with CO in chlorobenzene at 80 °C [equation (9)];[21] the reaction was also inhibited by added iodide.

$$[MeIr(CO)_2I_3]^- + CO \longrightarrow [(MeCO)Ir(CO)_2I_3]^- \qquad (9)$$

We have confirmed Forster's observations, and have obtained kinetic data for the carbonylation of **2b** using the high-pressure CIR cell (typical spectra are shown in Fig. 10). The activation parameters (Table 2), derived from rates measured in chlorobenzene over the temperature range 80–122 °C,* were independent of p_{CO} above a threshold of *ca.* 3.5 atm. A comparison between the metals can again be made: using the activation parameters for rhodium (k_2, see above) to predict a rate, under conditions comparable to those used for the iridium measurements, indicates that migration of methyl onto carbonyl is a factor of *ca.* 10^5 faster for rhodium(III) than for iridium(III) at 100 °C in an aprotic solvent. The slow rate of carbonylation of $[MeIr(CO)_2I_3]^-$ may also account for one potential problem that has been identified with iridium catalysts, namely that methane by-product formation is more significant.

Improvements in both the activity and selectivity of an iridium-catalysed process are therefore dependent on enhancing the rate of carbonylation of $[MeIr(CO)_2I_3]^-$. We have recently found that this reaction is dramatically accelerated on addition of small amounts of methanol, and to a somewhat smaller extent by higher alcohols (Fig. 11).[18] Further, kinetic measurements in a chlorobenzene–methanol (3:1) solvent system gave quite different activation parameters from those in neat chlorobenzene, with a much lower $\Delta H^\ddagger$ and a large negative $\Delta S^\ddagger$ (Table 2). These data suggest a change in the nature of the rate-determining step of the migration reaction from dissociative in neat chlorobenzene to associative in chlorobenzene–methanol. Our data for the model reaction are gratifyingly similar to those for the overall catalytic reaction in acetophenone–methanol, calculated from the rate data reported by Matsumoto.[16]

Addition of ionic iodide resulted in a decrease in rate, as previously reported by Forster.[21] These data are all consistent with the mechanism shown in Fig. 12, involving primary substitution of I^- by CO. We suggest that the iodide ligand *trans* to methyl is the most labile, and we note that in the crystal structure of the *n*-hexyl analogue (Fig. 6) the equivalent iodide (*trans* to hexyl) has the longest bond to iridium.

Thus, as for rhodium, but in a different context, methanol offers very large rate enhancements. In each case these appear

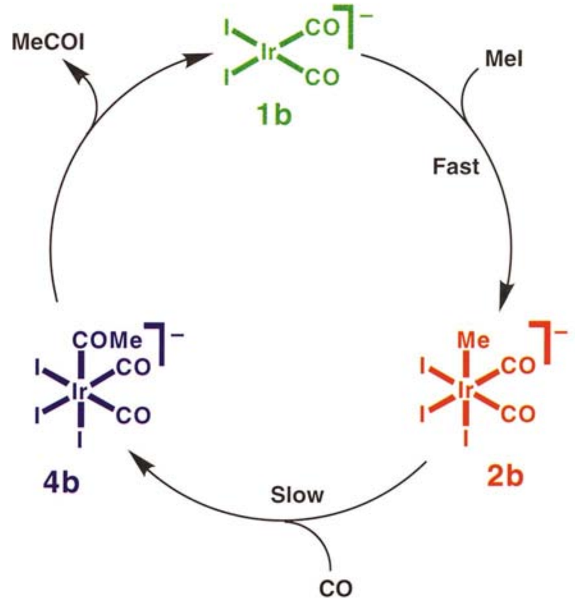

Fig. 9 A simplified catalytic cycle for carbonylation processes involving anionic iridium–carbonyl–iodide complexes. The organic reactions of MeI and MeCOI (shown in Fig. 1) are omitted for clarity

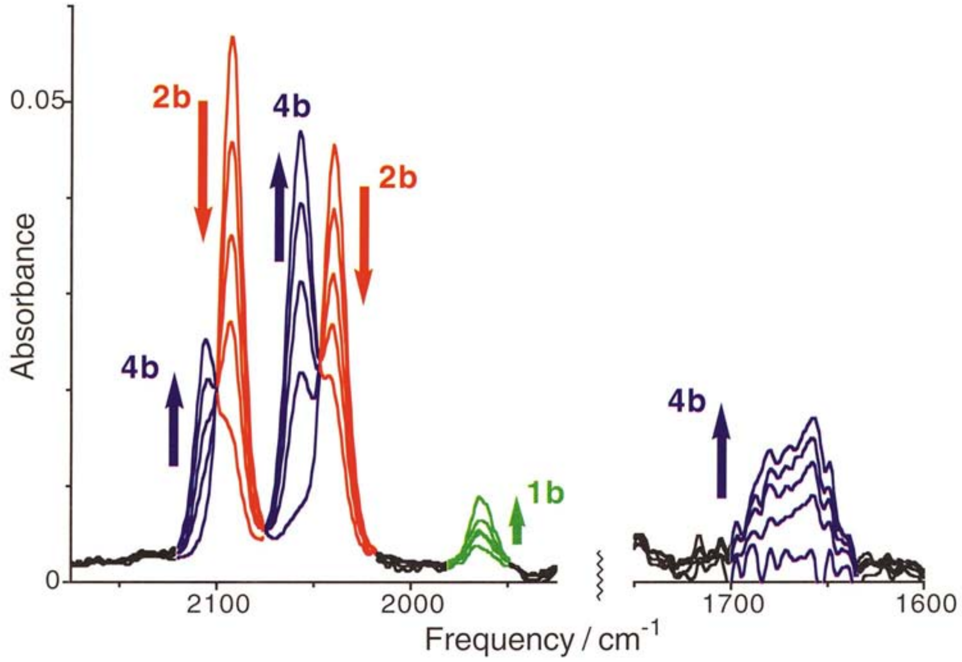

Fig. 10 A series of IR spectra illustrating the reaction of $[MeIr(CO)_2I_3]^-$ **2b** with carbon monoxide in chlorobenzene at 93 °C and 6 atm CO using the CIR cell

---

* For example, at 115 °C, 5 atm CO; $k_{obs} = ca.\ 2 \times 10^{-4}\ s^{-1}$.

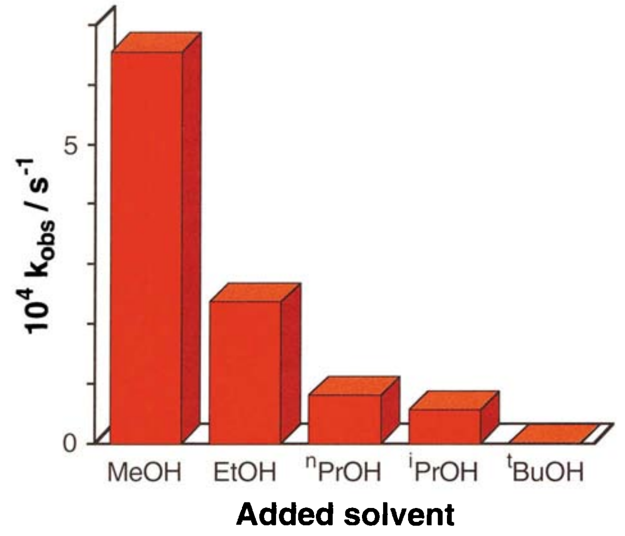

Fig. 11 The relative degrees of acceleration on the rate of carbonylation (5.7 atm CO) of $[MeIr(CO)_2I_3]^-$ **2b** effected by methanol and higher alcohols (25% v/v) in chlorobenzene at 33 °C

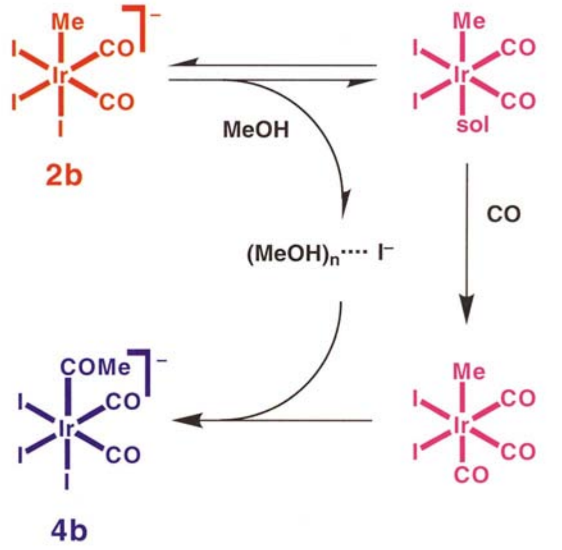

Fig. 12 Proposed mechanism for acceleratory effect of methanol on the carbonylation of complex **2b**

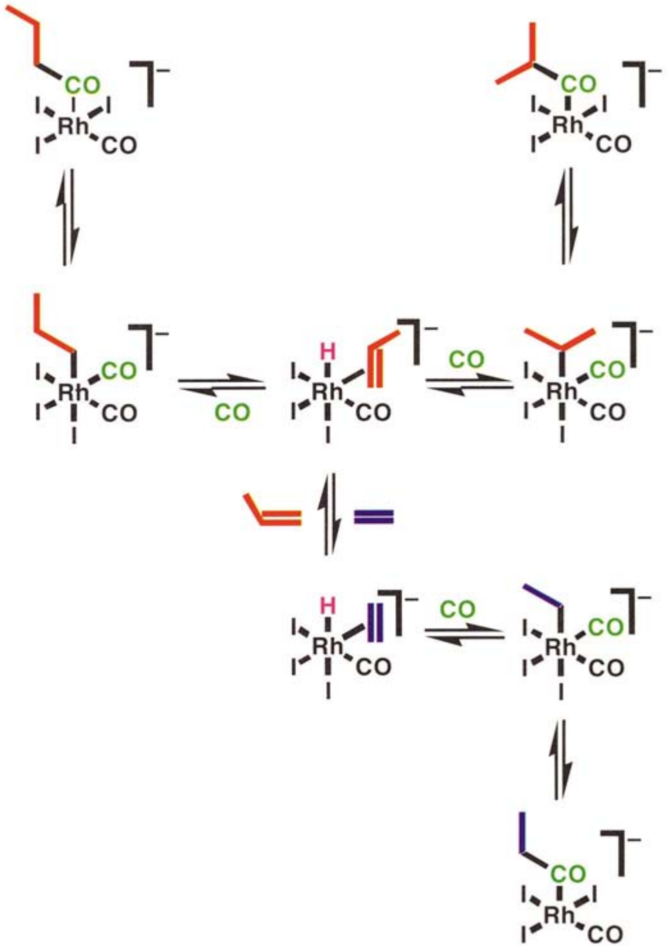

Fig. 13 Proposed mechanism for alkyl group isomerisation and alkene exchange reactions between rhodium(III) acyl complexes. The isomerisations lead to isomeric butanoic acids in the catalytic carbonylation of propanol

to be rather specific solvation effects; other authors have made similar observations.[25] It is also of interest that an excess of ionic iodide has opposite effects on the rate-determining steps for the rhodium and iridium processes. For rhodium, iodide has a beneficial effect on the oxidative addition reaction, whereas for iridium, added iodide inhibits the crucial migratory insertion step.

In view of the dramatic accelerations of migratory insertions induced by Lewis acids that Shriver and his collaborators have reported,[26] we also tested a range of metal iodides.[18] Significant acceleration of the migratory insertion was obtained for SnI_2, where we found that addition of 2 molar equivalents gave a rate enhancement of *ca.* 200, at 93 °C and 6 atm CO. Spectroscopic data suggested formation of an intermediate species, $[MeIr(CO)_2I_2(SnI_3)]^-$, which is activated for CO insertion. Extrapolation of data for the methanol-promoted reaction in chlorobenzene indicates a very similar rate enhancement at 93 °C, making the two promoters comparable. Thus, activation of an Ir–I bond in $[MeIr(CO)_2I_3]^-$ by methanol or by SnI_2 in the presence of CO leads to dramatic acceleration of migratory insertion.

Key Steps in Higher Alcohol Carbonylations

Rhodium- and iridium-iodide catalysts also promote the carbonylation of higher alcohols to linear or branched chain carboxylic acids,[27–29] for example, ethanol is converted into propanoic acid, and *n*-propanol yields a mixture of *n*- and *iso*-butanoic acids. Key steps in these catalytic cycles have also been investigated by our group.

The relative rates for the rhodium-catalysed carbonylations were found to decrease sharply in the order, methanol ≫ ethanol > propanol. Although $[Rh(CO)_2I_2]^-$ was very much less reactive towards the higher alkyl iodides than towards methyl iodide,[17] other key features of the stoichiometric reactions were similar: they gave the acyls $[(RCO)Rh(CO)I_3]^-$ as stable products [equation (10)],* and the rates were first order in [**1a**] and [RI].

$$RI + [Rh(CO)_2I_2]^- \longrightarrow [(RCO)Rh(CO)I_3]^- \qquad (10)$$

The mechanism of the alkyl isomerisation step in the rhodium reactions was investigated. The oxidative additions proceeded smoothly and cleanly at temperatures up to 80 °C with no evidence for alkyl group isomerisation. Further experiments showed that the isomerisation observed in the carbonylation of the higher alcohols occurs in the acyl complexes and a mechanism has been suggested (Fig. 13).

Recent work by the du Pont group has shown that $[(EtCO)Rh(CO)I_3]^-$ can also be generated by the reaction of $[Rh(CO)_2I_2]^-$ with HI and ethylene, the hydride $[HRh(CO)_2I_3]^-$ being detected as an intermediate at low temperature.[30] They suggested that this route may be favoured

---

* We suggest that the acyl complexes have the same dimeric structures in the solid state as was found for $[\{(MeCO)Rh(CO)I_3\}_2]^{2-}$.[5]

in the catalytic carbonylation of ethanol and of the higher alcohols. However, our activation parameters for oxidative addition of higher alkyl iodides are very similar to those for the corresponding alcohol carbonylations, suggesting that a route *via* ethylene may be of minor significance.

Addition of alkyl iodides to $[Ir(CO)_2I_2]^-$ was much faster than for the rhodium analogue, and proceeded under mild conditions (30 °C, 16 h, N_2 atmosphere) to give the alkyl complexes, $[RIr(CO)_2I_3]^-$. As for rhodium, reactions with higher alkyl iodides were much slower than with methyl iodide; again the reactions were first order in both [**1b**] and [RI].*

Comparison of oxidative addition kinetics for Rh and Ir gave the relative rates: $k_{Ir}/k_{Rh} = 150$ for MeI, 220 for EtI and 140 for Pr^{n}I (80 °C). The similarity in *relative* reactivity is understandable in view of the nearly identical radii of rhodium and iridium which lead to similar steric effects. For both metals the largest difference in reaction rate is observed between MeI and EtI, with much smaller changes on further increases in the alkyl chain length. Based on a rate arbitrarily chosen as 1000 for MeI, those for EtI are 3 for Rh and 2.3 for Ir. These values fall into the range reported for other transition-metal based nucleophiles,[31] where MeI is a factor of 10^2–10^3 more reactive than EtI. Non-transition-metal nucleophiles, such as iodide anion[32] and organic amines[33] also exhibit a large step change in reactivity between MeI (1000) and EtI (33), although the effect is somewhat less pronounced. The similarity in reactivity trends for all these reactions supports the proposal that oxidative addition to both Rh and Ir proceeds by a classic S_N2 process at carbon.[34] (Recent isotope effect measurements combined with *ab initio* calculations confirm this conclusion.) The greater difference in reactivity between methyl iodide and the longer chain alkyl iodides exhibited by metal complexes by comparison with organic nucleophiles, probably arises from steric congestion around the metal centre.

Relevance to Catalytic Alcohol Carbonylation

The relative rates for reaction of alkyl halides with $[Rh(CO)_2I_2]^-$ (MeI 1000, EtI 3, Pr^{n}I 1.7 and Pr^{i}I 4, all measured at, or extrapolated to, 80 °C) correlate reasonably well with the relative rates for the rhodium-catalysed carbonylation of the corresponding alcohols [1000 (MeOH), 48 (EtOH), 22 (Pr^{n}OH), 57–180 (Pr^{i}OH) at 170 °C and 35 atm CO]. The principal difference between the two series is the smaller step change in carbonylation rate between methanol and the higher alcohols, compared with the oxidative addition reactions. This may arise from the different temperatures and the different reaction media used in the two sets of experiments. The activation parameters obtained for the oxidative addition reactions also resemble those for catalytic carbonylation; the increase in $\Delta H^\ddagger$ for higher alkyls compared with methyl is similar for both catalytic carbonylation and oxidative addition (Table 2). Our data therefore fully support the conclusion that the oxidative addition step is also key in the rhodium–iodide catalysed carbonylation of the higher alcohols.

Conclusion

We have shown that catalytic carbonylation reactions can be analysed into a cyclic series of stoichiometric reactions, and that such analyses give useful information about the step in the cycle which determines the overall rate of the catalysis. There are, of course, some quantitative differences, which arise from the effects of different temperatures and different media in the two sets of experiments. However, the approach is clearly validated and one can now analyse other systems with reasonable confidence.

The key finding is that while $[Ir(CO)_2I_2]^-$ oxidatively adds organic iodides *ca.* 150 times faster than $[Rh(CO)_2I_2]^-$, migratory insertion on rhodium(III) is 10^5–10^6 faster than on iridium(III). One consequence of this is that whereas the alkyl–iridium(III)–carbonyl–iodide complexes are reasonably stable, the corresponding rhodium alkyls are very unstable and rapidly undergo migratory insertion to give the acyls. The increased stability of the alkyl–iridium complexes is probably a manifestation of the well known greater stability of the higher oxidation states for the 5d metals. Since the M–C bonds are in the same environments in the rhodium and the iridium complexes, the easier migration on rhodium may be a consequence of the relative strengths of the M–C bonds. Although no data are available for rhodium and iridium, bonds to 5d elements are generally stronger than those to the corresponding 4d metal.[35] Theoretical studies suggest that such differences arise principally from relativistic effects for the heavier metals.[36]

One can try to generalise the information available from these data. Thus, if a metal–ligand bond-making step plays a key role, then it is more likely that $k_{(5d)} > k_{(4d)}$; this is presumably what happens in the oxidative addition. By contrast, if a metal–ligand bond-weakening or -breaking step plays a key role in a process, such as the migration, it is likely that $k_{(4d)} > k_{(5d)}$.

Acknowledgements

It is a great pleasure to thank our colleagues and co-workers, Robb Watt and George Morris (BP Chemicals), Brian Mann, Cathryn Hickey, Tony Fulford, Jean Pearson and Paul Ellis in Sheffield, and Mauro Bassetti and Donato Monti in Rome, for their help in the work described in this article. We also thank BP Chemicals and the EPSRC (SERC) for support and the EU Human Capital and Mobility programme (Contract no. ERBCHRXCT930147) for additional assistance.

References

1 M. J. Howard, M. D. Jones, M. S. Roberts and S. A. Taylor, *Catal. Today*, 1993, **18**, 325.
2 R. T. Eby and T. C. Singleton, *Applied Industrial Catalysts*, ed. B. E. Leach, Academic Press, 1983, vol. 1, p. 275.
3 F. E. Paulik and J. E. Roth, *Chem. Commun.*, 1968, 1578; J. F. Roth, J. H. Craddock, A. Hershman and F. E. Paulik, *Chem. Technol.*, 1971, 600; K. K. Robinson, A. Hershman, J. H. Craddock and J. F. Roth, *J. Catal.*, 1972, **27**, 389; F. E. Paulik, A. Hershman, W. R. Knox and J. E. Roth, Monsanto Company, *US Pat.*, 3 769 329, 1973.
4 T. W. Dekleva and D. Forster, *Adv. Catal.*, 1986, **34**, 81.
5 G. W. Adamson, J. J. Daly and D. Forster, *J. Organomet. Chem.*, 1974, **71**, C17.
6 S. W. Polichnowski, *J. Chem. Educ.*, 1986, **63**, 204; V. H. Agreda, *Chem. Technol.*, 1988, 250; J. R. Zoeller, V. H. Agreda, S. L. Cook, N. L. Lafferty, S. W. Polichnowski and D. M. Pond, *Catal. Today*, 1992, **13**, 73.
7 See, for example, *Homogeneous Transition Metal Catalysed Reactions*, eds. W. R. Moser and D. W. Slocum, Advances in Chemistry Series 230, p. 3, and refs. therein.
8 A. Fulford, C. E. Hickey and P. M. Maitlis, *J. Organomet. Chem.*, 1990, **398**, 311.
9 A. Fulford and P. M. Maitlis, *J. Organomet. Chem.*, 1989, **366**, C20.
10 A. Haynes, B. E. Mann, D. J. Gulliver, G. E. Morris and P. M. Maitlis, *J. Am. Chem. Soc.*, 1991, **113**, 8567; A. Haynes, B. E. Mann, G. E. Morris and P. M. Maitlis, *J. Am. Chem. Soc.*, 1993, **115**, 4093.
11 H. Adams, N. A. Bailey, B. E. Mann, C. P. Manuel, C. M. Spencer and A. G. Kent, *J. Chem. Soc., Dalton Trans.*, 1988, 489.

---

* Although clean second-order kinetics were observed for the reaction of $[Ir(CO)_2I_2]^-$ with MeI, those with an excess of EtI and Pr^{n}I exhibited more complex kinetics, with substantial deviations from pseudo-first-order behaviour, particularly at higher temperatures in the presence of light or air. Addition of a radical scavenger restored simple kinetics, suggesting that the complex rate behaviour is due to a radical process which competes with the second-order reaction. We estimate that the radical component accounts for *ca.* 20% of the overall reaction of **1b** with ethyl iodide at 50 °C.

12 L. A. Howe and E. E. Bunel, *Polyhedron*, 1995, **14**, 167.

13 A. Haynes, D. Monti and P. M. Maitlis, unpublished work.

14 D. Forster, *J. Am. Chem. Soc.*, 1976, **98**, 846.

15 J. Hjortkjaer and O. R. Jensen, *Ind. Eng. Chem. Prod. Res. Dev.*, 1976, **15**, 46; J. Hjortkjaer and V. W. Jensen, *Ind. Eng. Chem. Prod. Res. Dev.*, 1977, **16**, 281; *J. Mol. Catal.*, 1978, **4**, 199.

16 D. Brodzki, B. Denise and G. Pannetier, *J. Mol. Catal.*, 1977, **2**, 149; T. Matsumoto, K. Mori and A. Ozaki, *J. Catal.*, 1978, **51**, 96; T. Mizoroki, T. Matsumoto and A. Ozaki, *Bull. Chem. Soc. Jpn.*, 1979, **52**, 479.

17 P. R. Ellis, J. M. Pearson, A. Haynes, H. Adams, N. A. Bailey and P. M. Maitlis, *Organometallics*, 1994, **13**, 3215.

18 J. M. Pearson, A. Haynes, G. E. Morris, G. J. Sunley and P. M. Maitlis, *J. Chem. Soc., Chem. Commun.*, 1995, 1045.

19 M. Schrod and G. Luft, *Ind. Eng. Chem. Prod. Res. Dev.*, 1981, **20**, 649; G. Luft and M. Schrod, *J. Mol. Catal.*, 1983, **20**, 175; 1983, **22**, 169; E. Lindner and B. Andre, *Chem. Ber.*, 1988, **121**, 829.

20 M. J. Baker, M. F. Giles, A. G. Orpen, M. J. Taylor and R. J. Watt, *J. Chem. Soc., Chem. Commun.*, 1995, 197; J. R. Dilworth, J. R. Miller, N. Wheatley, M. J. Baker and J. G. Sunley, *J. Chem. Soc., Chem. Commun.*, 1995, 1579.

21 D. Forster, *J. Chem. Soc., Dalton Trans.*, 1979, 1639.

22 D. Forster, *Inorg. Chem.*, 1972, **11**, 473.

23 J. M. Pearson, Ph.D. Thesis, University of Sheffield, 1994.

24 M. Bassetti, D. Monti, A. Haynes, J. M. Pearson, I. A. Stanbridge and P. M. Maitlis, *Gazz. Chim. Ital.*, 1992, **122**, 391.

25 O. Blum and D. Milstein, *J. Am. Chem. Soc.*, 1995, **117**, 4582.

26 S. B. Butts, S. H. Straus, E. M. Holt, R. E. Stimson, N. W. Alcock and D. F. Shriver, *J. Am. Chem. Soc.*, 1980, **102**, 5093; T. G. Richmond, F. Basolo and D. F. Shriver, *Inorg. Chem.*, 1982, **21**, 1272.

27 T. W. Dekleva and D. Forster, *J. Am. Chem. Soc.*, 1985, **107**, 3565, 3568; Abstract from the 187th National Meeting of the American Chemical Society, INDE 0108, 1984; *J. Mol. Catal.*, 1985, **33**, 269.

28 J. Hjortkjaer and J. C. Jorgensen, *J. Chem. Soc., Perkin Trans. 2*, 1978, 763; *J. Mol. Catal.*, 1978, **4**, 199.

29 S. B. Dake, D. S. Kohle and R. V. Chaudhari, *J. Mol. Catal.*, 1984, **24**, 99; S. B. Dake and R. V. Chaudhari, *J. Mol. Catal.*, 1986, **35**, 9119.

30 D. C. Roe, R. E. Sheridan and E. E. Bunel, *J. Am. Chem. Soc.*, 1994, **116**, 1163.

31 A. J. Hart-Davis and W. A. G. Graham, *Inorg. Chem.*, 1970, **9**, 2658; P. K. Monaghan and R. J. Puddephatt, *J. Chem. Soc., Dalton Trans.*, 1988, 595; G. N. Schrauzer and E. Deutsch, *J. Am. Chem. Soc.*, 1968, **90**, 2441.

32 J. Hine, *Physical Organic Chemistry*, McGraw-Hill, New York, 1962, p. 176.

33 J. March, *Advanced Organic Chemistry*, J. Wiley, New York, 4th edn., 1992, p. 339.

34 T. R. Griffin, D. B. Cook, A. Haynes, J. M. Pearson, D. Monti and G. E. Morris, *J. Am. Chem. Soc.*, 1996, **118**, 3029.

35 C. Mancuso and J. Halpern, *J. Organomet. Chem.*, 1992, **428**, C8.

36 T. Ziegler and V. Tschinke, *ACS Symp. Ser.*, 1990, 428.

Received 18*th December* 1995; *Paper* 5/08206D